Cavity Resonators - Theory & Possibilities for MRI

Andrew Webb. C.J.Gorter Centre for High Field MRI, Dept.Radiology, Leiden University Medical Centre, Albinusdreef 2, 2333 ZA Leiden, The Netherlands. a.webb@lumc.nl

Introduction

The majority of RF coils are formed from inductive lengths of copper in various geometries, which are tuned to resonance by incorporation of appropriate capacitors. Volume coils are based on geometries which have a (co)-sinusoidal variation in azimuthal current distribution to produce a homogeneous transverse RF field [1]. An alternative approach is to design a cavity resonator, in which the resonance frequency is determined by the material properties (in particular the relative permittivity) and the dimensions of the structure. Advantages of such designs include simplicity and robustness, the lack of multiple lumped elements, and very low losses. Such devices have found much use in electron paramagnetic resonance [2], but only with the advent of very high magnetic fields for human/animal/biochemical studies have the dimensions of cavity resonators become relevant for magnetic resonance. Historically, it is interesting to note that the probe used in the very first NMR experiments was a cavity resonator [3].

Theory

A cavity resonator is a very simple structure formed by a piece of hollow metal waveguide, with dimensions comparable to the wavelength, which is shorted at both ends. Normally the cavity is rectangular or cylindrical, as shown in Figure 1.

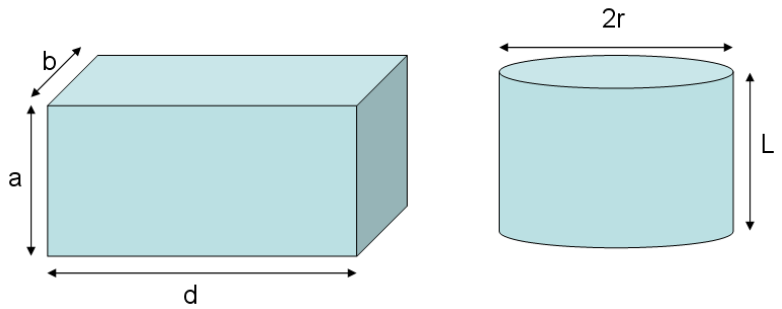

Figure 1. Basic geometries of (left) a rectangular cavity and (right) a cylindrical cavity.

Within such a cavity a large amount of energy can be stored in standing wave patterns arising from multiple reflections from the cavity walls, alternating between electric and magnetic fields which are 90° out-of-phase. There are a large number of different TE (Transverse Electric) modes and TM (Transverse Magnetic) modes. The subscripts m, n, and p represent the number of periodic half-waves in the x-, y-, and z-directions, respectively. For a rectangular waveguide the following equation describes the resonant frequencies of both TE_{mnp} and TM_{mnp} modes.

$$f = \frac{1}{2\sqrt{\mu_r \varepsilon_r}} \sqrt{\frac{m^2}{a^2} + \frac{n^2}{b^2} + \frac{p^2}{d^2}} \quad [1]$$

with m,n ,p being the mode numbers and a, b, d being the corresponding dimensions; μ and ε and are relative permeability and permittivity, respectively. For a rectangular cavity, the TM_{110} mode is the lowest possible mode, followed by either the TE_{101} or TE_{011} mode depending upon the particular geometry. TE modes are the most useful since the magnetic field is maximum at the centre of the cavity, which also corresponds to the volume of minimum electric field.

For a cylindrical cavity both TE and TM modes exist with resonance frequencies given by:

$$f_{TM} = \frac{1}{2\pi\sqrt{\mu\varepsilon}}\sqrt{\left(\frac{X_{mn}}{r}\right)^2 + \frac{p\pi}{L^2}} \qquad f_{TE} = \frac{1}{2\pi\sqrt{\mu\varepsilon}}\sqrt{\left(\frac{X'_{mn}}{r}\right)^2 + \frac{p\pi}{L^2}} \qquad [2]$$

defined in terms of Bessel functions $J_m(X_{mn})=0$ and $J'_m(X'_{mn})=0$.

From equation [1] we can calculate that, for example, an air-filled cubic metallic structure of dimensions 70 x 70x 70 cm would be necessary to resonate on a 7 Tesla system, and 53 x 53 x 53 cm at 9.4 Tesla! Dimensions are similarly unrealistic for air-filled cylindrical cavities. Therefore, we either need to think about dielectric-filled, or dielectric-based, cavity resonators, and/or more sophisticated geometries of cavity resonators: both approaches are considered in the following sections.

Metal-based cavities

A number of different cavity resonators have been proposed in the MRI literature, including toroidal [4-7], gapped-toroidal [8;9], and designs based on magnetroms [10-17].

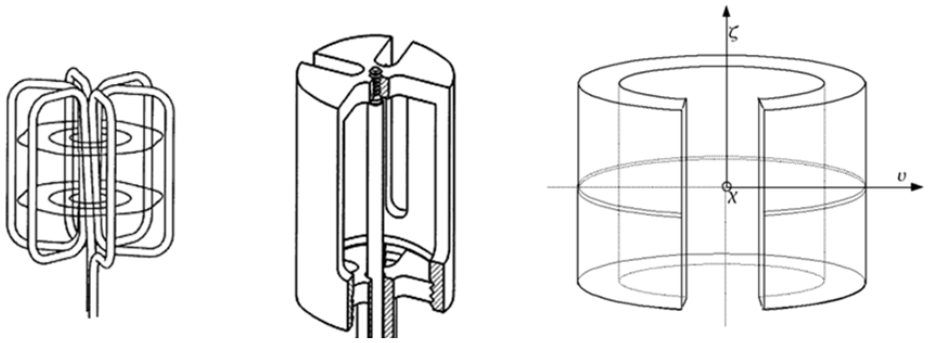

Figure 2. (left) The basic form of a toroidal coil made of a single piece of wire, in which the magnetic component of the RF field is entirely contained within the structure. (centre) A solid implementation of a toroid, with a shorted coaxial cable forming the central conductor [6]. (right) A gapped-toroid in which the sample is placed in the gap between the two shorted ends of the toroid [9].

The major disadvantage of such coils for standard NMR experiments is the variation in the radial field strength from the centre of the coil outwards, although the very strong B_1 gradient has been used for MR microscopy and RF-encoded diffusion measurements [5], as shown in Figure 3.

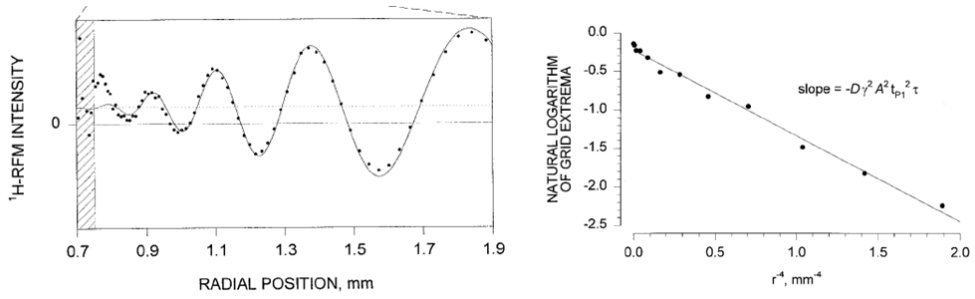

Figure 3. (left) The dependence of signal intensity on radial position for a toroidal coil [5]. (right) Measurements of diffusion coefficients using the RF gradient and a MAGROFI [18] pulse sequence.

TEM and re-entrant cavities

The TEM coil of Vaughan et al. [19;20] has found extensive use, particularly at high fields, and consists of a coaxial cavity, which can also be considered as a coaxial line shorted at two ends and joined in the centre by a capacitor. In practice the central capacitor is split into a set of parallel coaxial rods. Thus, the largely inductive coaxial line (cavity) is shorted on both ends, and is resonated with primarily-capacitive open ended coaxial line elements. Re-entrant cavity designs are based upon back-to-back coaxial re-entrant cavities which are bridged by a series of parallel structures, with appropriate tuning capacitors [21].

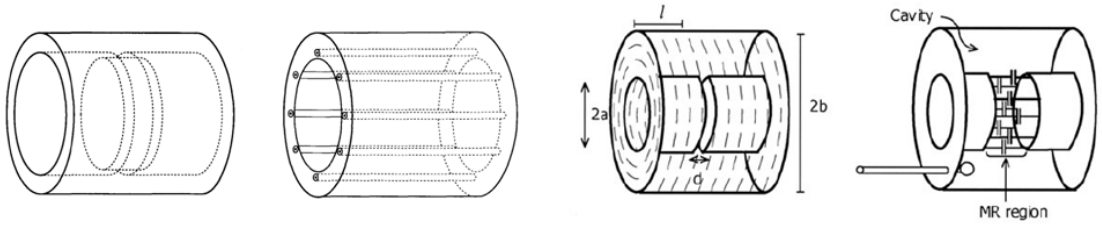

Figure 4. (left) Basic form of a coaxial cavity and its realization as a TEM cavity resonator. (right) Corresponding form of a re-entrant cavity, and its MR-relevant equivalent.

Dielectric cavity resonators

Cavities can also be formed from materials with high dielectric constant, which require no lumped elements. The field distribution in dielectric cavity resonators is similar to the field distribution in hollow metal resonators of the same shape if the difference between the permittivity of the resonator and that of the surrounding space is large. For a cylindrical resonator with radius a and height h, the two lowest frequency modes are the $TE_{01\delta}$ and $HEM_{11\delta,}$ with the respective values given by:

$$f_{TE_{01\delta}} = 2.921\frac{c\varepsilon_r^{-0.465}}{2\pi a}\left[0.691+0.319\frac{a}{h}-0.035\left(\frac{a}{h}\right)^2\right] \quad [3]$$

$$f_{HEM_{11\delta}} = 2.735 \frac{c\varepsilon_r^{-0.436}}{2\pi a}\left[0.543 + 0.589\frac{a}{h} - 0.05\left(\frac{a}{h}\right)^2\right] \qquad [4]$$

The field patterns of the two modes are shown below.

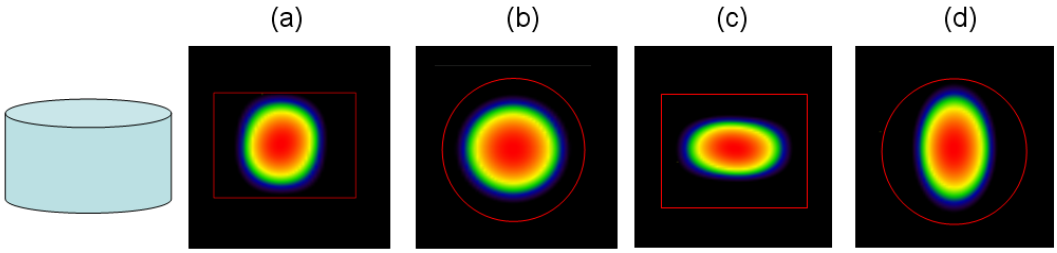

Figure 5. Transverse and axial views of the B_1^+ fields from a circular dielectric cavity resonator. (a) and (b) $TE_{01\delta}$ mode, (c) and (d) one of the degenerate $HEM_{11\delta}$ modes.

By perturbation theory it can be shown that the field patterns are not distorted significantly by the introduction of a central hole for sample access. Clearly the $TE_{01\delta}$ mode can be used only with the height-axis aligned perpendicular to the B_0 field, and therefore is of limited practicality for in vivo imaging [22], although for ex vivo samples the sample itself can act as a resonator [23]. In contrast, the two degenerate $HEM_{11\delta}$ mode can be used with the height-axis parallel to B_0, and driven in quadrature. Aussenhofer et al. have used degenerate circularly-polarized HEM_{11} modes to image the wrist at 7T (298.1 MHz), with water as the dielectric [24], with in vivo images shown in Figure 6.

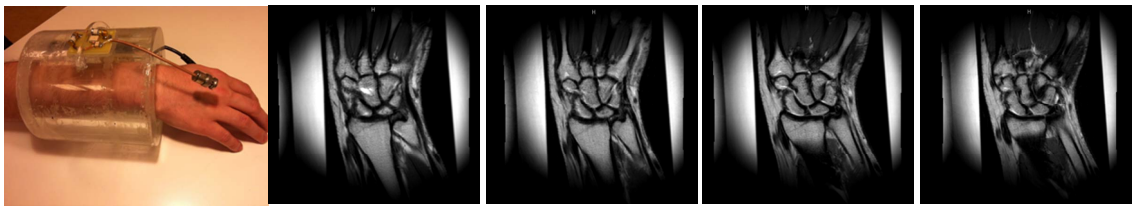

Figure 6. (left) A quadrature HEM_{11} resonator with two inductive coupling loops used for impedance matching. (right) Adjacent slices from the human wrist using the water-based cavity resonator.

In MR microimaging the higher frequencies (400-900 MHz) in combination with the smaller diameter magnet bore means that high permittivity materials need to be used. Neuberger et al. [25] used ceramic discs of barium strontium titanate, which has a relative permittivity of 323, on a vertical bore 14.1 T (600 MHz) system. An alternative material for a DR is $CaTiO_3$, ϵ_r value 156, which is much more widely available at lower cost [26].

From cavities to waveguides - travelling wave experiments.

By removing the end caps from a cavity, one obtains a metallic waveguide structure, which can support different travelling, as opposed to standing, wave modes. TE and TM modes both exhibit cut-off frequencies, ie a frequency below which a standing wave mode cannot be formed. The intriguing area of travelling wave excitation [27-29], discussed in detail in the next lecture, relies on the fact that the cutoff frequency for the TE_{11} mode is just lower than the Larmor frequency for 7 Tesla systems loaded with the human body, and significantly lower for 9.4 Tesla, at which field the TM_{01} mode can also propagate. The propagation properties of these modes can be significantly affected by the insertion of dielectric cavity resonators, with the fields able to be steered and concentrated, neatly combining the worlds of waveguides and cavities.

References

[1] C.E. Hayes, The development of the birdcage resonator: a historical perspective. Nmr in Biomedicine 22 (2009) 908-918.

[2] G. Annino, M. Cassettari, I. Longo, M. Martinelli, Dielectric resonators in ESR: Overview, comments and perspectives. Applied Magnetic Resonance 16 (1999) 45-62.

[3] R.V. Pound, From radar to nuclear magnetic resonance. Reviews of Modern Physics 71 (1999) S54-S58.

[4] J.W. Rathke, R.J. Klingler, R.E. Gerald, K.W. Kramarz, K. Woelk, Toroids in NMR spectroscopy. Progress in Nuclear Magnetic Resonance Spectroscopy 30 (1997) 209-253.

[5] K. Woelk, R.E. Gerald, R.J. Klingler, J.W. Rathke, Imaging diffusion in toroid cavity probes. Journal of Magnetic Resonance Series A 121 (1996) 74-77.

[6] K. Woelk, J.W. Rathke, R.J. Klingler, The Toroid Cavity Nmr Detector. Journal of Magnetic Resonance Series A 109 (1994) 137-146.

[7] K. Woelk, J.W. Rathke, R.J. Klingler, Rotating-Frame Nmr Microscopy Using Toroid Cavity Detectors. Journal of Magnetic Resonance Series A 105 (1993) 113-116.

[8] E.J. Butterworth, J.C. Gore, Computing the B-1 field of the toroidal MRI coil. J.Magn.Reson. 175 (2005) 114-123.

[9] E.J. Butterworth, E.G. Walsh, J.W. Hugg, TiO2 dielectric filled toroidal radio frequency cavity resonator for high-field NMR. Nmr in Biomedicine 14 (2001) 184-191.

[10] P. Mansfield, M. Mcjury, P. Glover, High-Frequency Cavity Resonator Designs for Nmr. Measurement Science & Technology 1 (1990) 1052-1059.

[11] P. Mansfield, The Petal Resonator - A New Approach to Surface Coil Design for Nmr Imaging and Spectroscopy. Journal of Physics D-Applied Physics 21 (1988) 1643-1644.

[12] O. Marrufo, F. Vasquez, S.E. Solis, A.O. Rodriguez, Slotted cage resonator for high-field magnetic resonance imaging of rodents. Journal of Physics D-Applied Physics 44 (2011).

[13] A.O. Rodriguez, S.S. Hidalgo, R. Rojas, F.A. Barrios, Experimental development of a petal resonator surface coil. Magnetic Resonance Imaging 23 (2005) 1027-1033.

[14] A.O. Rodriguez, S.E. Solis, M.A. Lopez, M.C. Mantaras, S.S. Hidalgo, Performance of a petal resonator surface (PERES) coil via equivalent circuit simulation. Revista Mexicana de Fisica 52 (2006) 398-403.
[15] A.O. Rodriguez, Magnetron surface coil for brain MR imaging. Archives of Medical Research 37 (2006) 804-807.
[16] A.O. Rodriguez, S.S. Hidalgo, R. Rojas, F.A. Barrios, A petal resonator volume coil for MR neuroimaging. Revista Mexicana de Fisica 52 (2006) 272-277.
[17] S.E. Solis, R. Wang, D. Tomasi, A.O. Rodriguez, A multi-slot surface coil for MRI of dual-rat imaging at 4 T. Physics in Medicine and Biology 56 (2011) 3551-3561.
[18] R. Kimmich, B. Simon, H. Kostler, Magnetization-Grid Rotating-Frame Imaging Technique for Diffusion and Flow Measurements. Journal of Magnetic Resonance Series A 112 (1995) 7-12.
[19] J.T. Vaughan, H.P. Hetherington, J.O. Otu, J.W. Pan, G.M. Pohost, High frequency volume coils for clinical NMR imaging and spectroscopy. Magn Reson.Med 32 (1994) 206-218.
[20] J.T. Vaughan, G. Adriany, C.J. Snyder, J. Tian, T. Thiel, L. Bolinger, H. Liu, L. DelaBarre, K. Ugurbil, Efficient high-frequency body coil for high-field MRI. Magn Reson.Med. 52 (2004) 851-859.
[21] B.L. Beck, K.A. Jenkins, J.R. Fitzsimmons, Geometry comparisons of an 11-T coaxial reentrant cavity (ReCav) coil. Concepts in Magnetic Resonance Part B-Magnetic Resonance Engineering 18B (2003) 24-27.
[22] H. Wen, F.A. Jaffer, T.J. Denison, S. Duewell, A.S. Chesnick, R.S. Balaban, The evaluation of dielectric resonators containing H_2O or D_2O as RF coils for high-field MR imaging and spectroscopy. J.Magn.Reson.Ser.B 110 (1996) 117-123.
[23] A.G. Webb, Visualization and characterization of pure and coupled modes in water-based dielectric resonators on a human 7T scanner. J.Magn.Reson. 216 (2012) 107-113.
[24] S.A. Aussenhofer, A.G. Webb, Design and evaluation of a detunable water-based quadrature HEM11 mode dielectric resonator as a new type of volume coil for high field MRI. Magnetic Resonance in Medicine 68 (2012) 1325-1331.
[25] T. Neuberger, V. Tyagi, E. Semouchkina, M. Lanagan, A. Baker, K. Haines, A.G. Webb, Design of a ceramic dielectric resonator for NMR microimaging at 14.1 tesla. Concepts in Magnetic Resonance Part B-Magnetic Resonance Engineering 33B (2008) 109-114.
[26] K. Haines, T. Neuberger, M. Lanagan, E. Semouchkina, A.G. Webb, High Q calcium titanate cylindrical dielectric resonators for magnetic resonance microimaging. J Magn Reson. 200 (2009) 349-353.
[27] D.O. Brunner, Z.N. De, J. Frohlich, J. Paska, K.P. Pruessmann, Travelling-wave nuclear magnetic resonance. Nature 457 (2009) 994-998.
[28] A.G. Webb, C.M. Collins, M.J. Versluis, H.E. Kan, N.B. Smith, MRI and localized proton spectroscopy in human leg muscle at 7 Tesla using longitudinal traveling waves. Magn Reson Med 63 (2010) 297-302.
[29] B. Zhang, D.K. Sodickson, R. Lattanzi, Q. Duan, B. Stoeckel, G.C. Wiggins, Whole body traveling wave magnetic resonance imaging at high field strength: Homogeneity, efficiency, and energy deposition as compared with traditional excitation mechanisms. Magnetic Resonance in Medicine 67 (2012) 1183-1193.